

On-Chip Near-Field Electromagnetic Shielding Effect of Electroplated Copper Layers

Tae Goo Kang and Young-Ho Cho*

Digital Nanolocomotion Center, Micromachines and Microsystems Laboratory
Korea Advanced Institute of Science and Technology
373-1 Guseong-dong, Yuseong-gu, Daejeon 305-701, Republic of Korea

(Received September 18, 2000; accepted January 28, 2002)

Key words: microwave transceiver, near-field electromagnetic shielding, on-chip shielding packaging, multi-chip microsystems, electroplated copper

Near-field electromagnetic loss of electroplated copper layers has been characterized for applications to multichip microsystems with on-chip electromagnetic protection. Copper layers in the thickness range of $0.2\ \mu\text{m}$ – $200\ \mu\text{m}$ have been electroplated on Pyrex glass substrates. A pair of microwave transceivers $3.5\ \text{mm} \times 3.5\ \text{mm}$ in size has been fabricated using electroplated nickel microloop antennas. An electromagnetic radiation loss of 10 dB–40 dB has been measured from the copper layers in the thickness range of $0.2\ \mu\text{m}$ – $200\ \mu\text{m}$ for the wave bandwidth of 100 MHz ~ 1 GHz. The $0.2\text{-}\mu\text{m}$ -thick copper layer provides a shield loss of 20 dB at frequencies higher than 300 MHz while showing a predominant decrease of shield loss to the 10 dB level at lower frequencies. No substantial increase of shield effectiveness has been observed for copper shield layers thicker than $2\ \mu\text{m}$.

1. Introduction

Recently, the micro-electromechanical system (MEMS) has been developed for an integrated microsystem⁽¹⁾ with applications to low-power, high-density and multifunctional devices. Particularly for applications in information and communications fields, the microsystem requires multi-chip integration of the inductive elements^(2,3) or capacitive devices which are sensitive to electromagnetic interference. Thus microdevice packaging with an on-chip shield layer (Fig. 1) provides a promising solution for multichip systems containing noise-sensitive devices and noise sources.

In the previous MEMS packaging research, metal layers were used to protect electronic

* Corresponding author, e-mail address: mems@kaist.ac.kr

devices from the high anodic bonding voltage⁽⁴⁾ as well as to shield capacitive devices sensitive to illumination current.⁽⁵⁾ In this paper, however, we describe the use of electroplated copper layers as electromagnetic shield media for on-chip electromagnetic encapsulation.

We fabricated a set of electroplated copper layers in the thickness range of $0.2 \mu\text{m} \sim 200 \mu\text{m}$. Using a pair of electroformed nickel microloop transceivers, the electromagnetic shielding effectiveness of the copper layers has been measured and evaluated in the bandwidth of 100 MHz~1 GHz.

2. Near-Field Electromagnetic Loss

Figure 2 shows an electromagnetic shield model where the electromagnetic wave passes through the shield. We focus on the near-field when the distance from the electromagnetic source to the shield is much smaller than the characteristic distance of $\lambda/2\pi$.

For an electromagnetic wave of the frequency ω , the impedance of the medium is described⁽⁶⁾ as

$$Z_o = \sqrt{\frac{j\omega\mu}{\sigma + j\omega\epsilon}} \quad (1)$$

where μ , ϵ and σ are the permeability, dielectric constant and conductivity of the medium, respectively.

For insulators, the medium impedance is expressed by

$$Z_o = \sqrt{\mu/\epsilon} \quad (2)$$

For air or free space, an impedance of $Z_o = 377 \Omega$ is obtained using the values of $4\pi \times 10^{-7}$ H/m and $\epsilon = 8.85 \times 10^{-12}$ F/m.

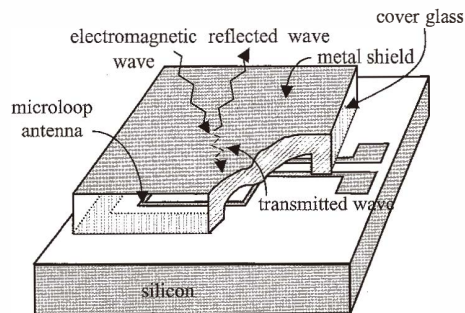


Fig. 1. On-chip electromagnetic shield of the microloop antenna using the cover glass with electroplated metal layer.

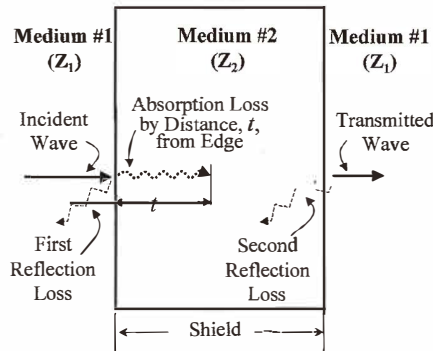


Fig. 2. An electromagnetic shield model for a wave passing through the shield.

For conductors, the magnitude of the shield impedance, Z_s , is reduced to

$$Z_s = \sqrt{\omega\mu / \sigma} . \tag{3}$$

For copper, the shield impedance is obtained as

$$Z_s = 3.68 \times 10^{-7} \sqrt{f} , \tag{4}$$

where a relative permeability of $\mu_r = 1$ and a conductivity of $\sigma = 5.82 \times 10^7$ mho/m are assumed, and f presents the wave frequency. In the frequency range of 100 MHz ~ 1 GHz, the shield impedance of copper ranges from $3.68 \times 10^{-3} \Omega$ (at 100 MHz) to $11.6 \times 10^{-3} \Omega$ (at 1 GHz).

The skin depth of the shield is defined as the distance required for the wave to be attenuated to $1/e$ or 37% of its original wave and is described⁽⁶⁾ as

$$\delta = \sqrt{2 / \omega\mu\sigma} \text{ [m]} . \tag{5}$$

For copper, the skin depth is expressed by

$$\delta = \frac{66040}{\sqrt{f\mu_r\sigma_r}} \text{ [\mu m]} , \tag{6}$$

where σ_r is a relative conductivity, thus providing a skin depth range of $6.6 \mu\text{m} \sim 2.1 \mu\text{m}$ in the wave frequency range of 100 MHz ~ 1 GHz.

Near-field shielding effectiveness or shield loss⁽⁶⁾ is considered as the sum of the absorption loss, A , the reflection loss, R , and the correction factor or multiple reflection loss, B , as follows.

$$S = A + R + B \quad [\text{dB}] \quad (7)$$

The absorption loss, A , is proportional to the ratio of the medium thickness, t , and the skin depth, δ , as shown in eq. (8):

$$A = 1.315 \times 10^{-4} t \sqrt{f \mu_r \sigma_r} \quad [\text{dB}], \quad (8)$$

where t is the medium thickness in micrometers.

The reflection loss at the interface between two media is related to the difference in characteristic impedance between them. The reflection loss, R , can be written as⁽⁶⁾

$$R = 20 \log \frac{|Z_w|}{4|Z_s|} \quad [\text{dB}], \quad (9)$$

where Z_w and Z_s are the wave impedance for Z_1 and shield impedance for Z_2 in Fig. 2, respectively. The wave impedance of the magnetic field can be approximated by the following equation when $r < \lambda/2\pi$:

$$|Z_w|_m = 2\pi f \mu r, \quad (10)$$

where r is the distance from the source to the shield. The reflection loss can be determined by substituting eq. (10) and eq. (3) into eq. (9) as follows:

$$R = 14.6 + 10 \log \left(\frac{\sigma_r r^2 f}{\mu_r} \right) \quad [\text{dB}], \quad (11)$$

where μ_r and σ_r denote the relative permeability and the relative conductivity of the shield, respectively. The terms f and r in eq. (11) indicate the frequency of the wave and the distance from the source to the shield in meters, respectively. The correction factor, B , is considered to account for multiple reflections in thin shields and is defined as

$$B = 20 \log(1 - e^{-2t/\delta}) \quad [\text{dB}]. \quad (12)$$

3. Test Structure and Experimental Setup

We fabricated four different sets of copper shield layers having thicknesses of $0.2\ \mu\text{m}$, $2\ \mu\text{m}$, $21\ \mu\text{m}$ and $200\ \mu\text{m}$. Each copper layer was electroplated on a Cr/Cu seed layer evaporated on $500\text{-}\mu\text{m}$ -thick Pyrex glass substrate. We have also fabricated a nickel microloop antenna (Fig. 3), for use in the electromagnetic transceivers that generate and receive electromagnetic radiation.

Figure 4 shows the fabrication process for the microloop antenna. The fabrication process starts with the deposition of a $2500\text{-}\text{\AA}$ -thick low-pressure chemical vapor deposition (LPCVD) Si_3N_4 (Fig. 4(a)) insulating layer on the silicon wafer. In Fig. 4(a), a $0.1\text{-}\mu\text{m}$ -thick Cr/Cu composite layer is evaporated on the nitride layer as a seed layer for the nickel electroplating process. A $15\text{-}\mu\text{m}$ -thick photoresist (PR) is coated and patterned (Fig. 4(b)) to obtain the PR mold for the microloop antenna. The nickel electroplating process (Fig. 4(c)) using the PR mold results in the selective filling or forming of a nickel structure within the mold. After the removal of the Cr/Cu layer (Fig. 4(d)) covered by PR, we obtain the nickel microloop antenna (Fig. 3) having a total loop length of $15\ \text{mm}$.

The pair of microtransceivers illustrated in Fig. 5(a) has been assembled on a printed circuit board (PCB) using the microloop antenna chip attached to a ceramic dual-in-line (DIP) package. The microtransceiver packages of Fig. 5(a) are covered by a grounded copper case having a square opening over the microloop antenna area, thus resulting in the microtransceiver module shown in Fig. 5(b).

Figure 6 illustrates the experimental setup for the measurement of electromagnetic loss in the copper layers. The electroplated copper layers have been placed between a pair of microtransceiver modules (Fig. 5) where the upper module is used as a receiver and the lower module as a transmitter. The radiation power loss across the copper shield layers was monitored by the network analyzer in the frequency range of $100\ \text{MHz} \sim 1\ \text{GHz}$.

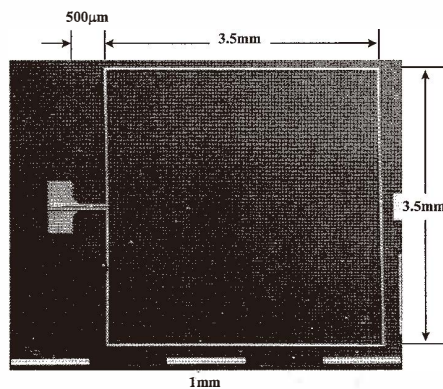


Fig. 3. SEM image of the microfabricated nickel microloop antenna for use in electromagnetic transceivers: a $20\text{-}\mu\text{m}$ -wide, $12\text{-}\mu\text{m}$ -thick, 15-mm -long nickel loop was electroformed on the silicon wafer.

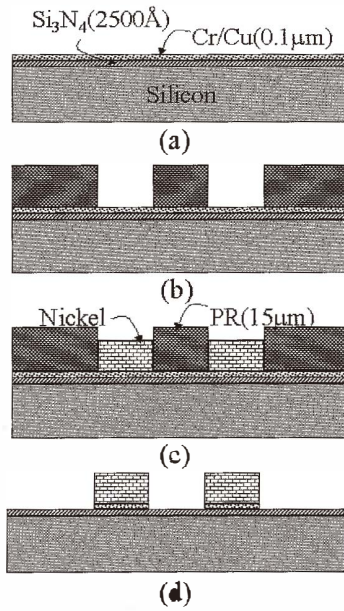


Fig. 4. Microfabrication process for the nickel microloop antenna.

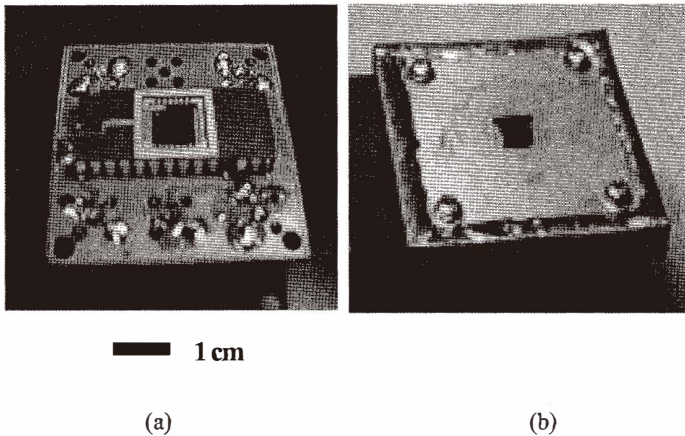


Fig. 5. Photograph of the microtransceiver using a nickel microloop antenna: (a) the microtransceiver where the microloop antenna chip is attached to the DIP packages on a PCB board, (b) the microtransceiver shielded by a grounded copper case having a square opening above the microloop antenna chip.

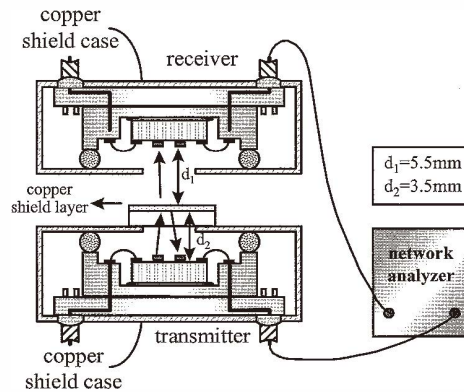


Fig. 6. Measurement of the electromagnetic radiation passing through the glass cover with an electroplated copper shield layer.

4. Results and Discussion

In our experimental case, the characteristic distance $\lambda/2\pi$ is in the range of 47.7 m ~ 47.7 mm for the frequency range of 100 MHz ~ 1 GHz. The distance from the electromagnetic source to the shield ($r = 3.5$ mm) is much smaller than the characteristic length, thus corresponding to the near-field problem.

The network analyzer compares the power detected by the receiver and that supplied to the transmitter, resulting in the power measurement in Fig. 7 for different shielding layers in the electromagnetic wave frequency range of 100 MHz ~ 1 GHz. We repeated the measurement of the radiation power loss across the transceivers three times for each shield layer and averaged the values to obtain Fig. 7(a). Table 1 compares the theoretical values estimated by eqs. (6) ~ (7) and the experimental values extracted from Fig. 7(b).

From Fig. 7(a), we found that neither silicon wafer or Pyrex glass can serve as electromagnetic shielding materials. The shielding effectiveness, shown in Fig. 7(b), was obtained by subtracting the measured power signals for the silicon wafer from the measured values in Fig. 7(a).

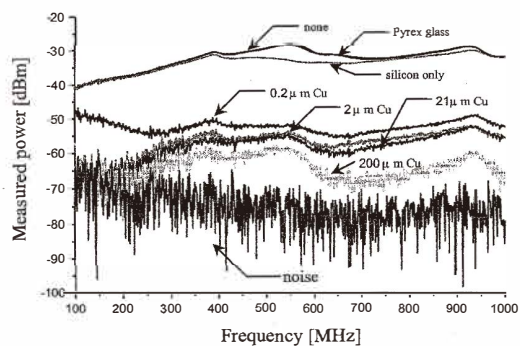
From Fig. 7(b), we find that the electromagnetic shielding effect of the copper layer tends to increase with wave frequency and layer thickness. Particularly for the 0.2- μm -thick copper layer, the decrease in the shielding effect is dominant at lower frequencies due to the multiple reflection effect.

It is also noted from Fig. 7(b) that, at the higher frequencies, the thickness of the copper layer has only a small effect on the electromagnetic shielding. The 200- μm -thick copper layer, for example, provides only a 10 dB increase in the shielding effect compared with a 0.2- μm -thick layer. The small dependence of shield thickness on the measured shielding effect might be caused by the electromagnetic radiation passing around the edge of the shield layer of 8 mm \times 8 mm size. The 0.2- μm -thick copper layer, however, provides a measured electromagnetic shield effect of 20 dB, showing the potential for on-chip electromagnetic shielding applications.

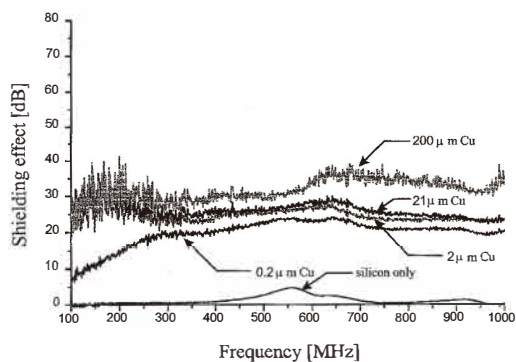
Table 1

Estimated and measured characteristics of the copper shield having a thickness, t , and a skin depth, d , in the wave bandwidth range of 100 MHz ~ 1 GHz.

t [μm]	t/d	estimated loss [dB]	measured loss [dB]
0.2	0.030 ~ 0.096	21.13 ~ 41.13	20 ± 3
2	0.30 ~ 0.96	41.27 ~ 52.41	25 ± 3
21	3.18 ~ 10.0	72.79 ~ 142.8	26 ± 3
200	30.3 ~ 95.7	308.5 ~ 887.2	32 ± 3



(a)



(b)

Fig. 7. Measured radiation and shielding effectiveness: (a) radiation passing through the copper shield layers, (b) electromagnetic shielding effectiveness of the copper layers.

5. Conclusions

We carried out an experimental investigation on the near-field electromagnetic loss of thin copper layers for applications to multichip microsystems with on-chip electromagnetic protection. We fabricated the electroplated copper shield layers in the thickness range of $0.2\ \mu\text{m} \sim 200\ \mu\text{m}$ and a set of electromagnetic microtransceivers using the electroformed nickel microloop antennas. The measured effectiveness of the copper shield layers was in the range of 10 dB \sim 40 dB for the frequency range of 100 MHz \sim 1 GHz. The $0.2\text{-}\mu\text{m}$ -thick copper layer provides a shield loss of 20 dB at frequencies higher than 300 MHz, whereas it shows a predominant decrease in shield loss to 10 dB level at lower frequencies. No substantial increase in shield effectiveness has been found for copper shield layers thicker than $2\ \mu\text{m}$. The discrepancy between the theoretical estimation and the experimental measurement seems to be caused by the effect of shield geometry⁽⁶⁾ which enables electromagnetic radiation to pass through or around a shield layer of finite size. The $0.2\text{-}\mu\text{m}$ -thick copper layer, however, provides an electromagnetic shield effect of 20 dB, showing the potential for on-chip electromagnetic shielding applications. The proposed on-chip metal shield encapsulation is a feasible method for chip-level protection of susceptible devices, such as integrated microsensors sensitive to electromagnetic environments, while maintaining the integrity of multichip modules.

Acknowledgement

This work was conducted by "Digital Nanolocomotion Center", a Creative Research Initiative Program of the Ministry of Science and Technology. The authors also acknowledge the assistance of Mr. Jonghoon Kim in the testing and measurement processes as well as technical discussions with Professor Joungho Kim in the Department of Electrical Engineering, KAIST.

References

- 1 Y. B. Gianchandani, K. J. Ma and K. Najafi: Tech. Digest of Transducers '95 (Stockholm 1995) p. 79.
- 2 C. T.-C. Nguyen: Proc. IEEE Workshop on Micro Electro Mechanical Systems (Heidelberg 1998) p. 1.
- 3 S. Shoji, H. Kikuchi and H. Torigoe: Proc. IEEE Workshop on Micro Electro Mechanical Systems (Nagoya 1997) p. 482.
- 4 K. Baert, L. Deferm, P. Jansen, M. Rosmeulen and S. van der Groen: 5th Inter. Conf. Micro Electro, Opto, Mechanical Systems and Components (Potsdam 1996) p. 762.
- 5 M. Esashi: Tech. Digest of Transducers '93 (Yokohama 1993) p. 260.
- 6 H. W. Ott: Noise Reduction Techniques in Electronic Systems, 2nd ed. (John Wiley & Sons, 1987) p. 159.

About the Authors

Tae Goo Kang was born in Taegu, Korea, in 1972. He received a B.S. degree and a M.S. degree from the Department of Mechanical Engineering at the Korea Advanced Institute of Science and Technology (KAIST) in 1994 and 1997, respectively. His research interests are focused on microfluidic systems and microsystem packaging. Currently, he is working on microinjector systems for his Ph.D.

Young-Ho Cho received the B.S. degree *summa cum laude* from Yeungnam University, Taegu, Korea, in 1980, the M.S. degree from the Korea Advanced Institute of Science and Technology (KAIST), Seoul, Korea, in 1982, and the Ph.D. degree from the University of California at Berkeley for his MEMS work completed in December, 1990.

From 1982 to 1986 he was a Research Scientist of CAD/CAM Research Laboratory, Korea Institute of Science and Technology (KIST), Seoul, Korea. During 1987–1991, he worked as a Graduate Student Researcher (1987–1990) and then a Post-doctoral Researcher (1991) of the Berkeley Sensor and Actuator Center at the University of California at Berkeley. In August 1991, Dr. Cho moved to KAIST, where he is currently an Associate Professor in the Department of Mechanical Engineering.

Dr. Cho's research interests are focused on the development of inertial microsensors, micromechanical actuators, and opto-/thermo-fluidic- micromechanical components for applications to automotive electronics systems, inertial navigation systems, information and communication systems, and other devices. He has served as the Chair of the Steering Committee for Korea National MEMS Programs as well as a member of the Program Committee for international MEMS conferences, including the IEEE MEMS Conference and the IEEE MOEMS Conference. Dr. Cho is a member of IEEE and ASME.